

XP-000952187

## Subunit organization of the abalone *Haliotis tuberculata* hemocyanin type 2 (HtH2), and the cDNA sequence encoding its functional units d, e, f, g and h

Bernhard Lieb, Benjamin Altenhein, Rolf Lehnert, Wolfgang Gebauer and Jürgen Markl

Institute of Zoology, University of Mainz, Germany

We have developed a HPLC procedure to isolate the two different hemocyanin types (HtH1 and HtH2) of the European abalone *Haliotis tuberculata*. On the basis of limited proteolytic cleavage, two-dimensional immunoelectrophoresis, PAGE, N-terminal protein sequencing and cDNA sequencing, we have identified eight different 40–60-kDa functional units (FUs) in HtH2, termed HtH2-a to HtH2-h, and determined their linear arrangement within the elongated 400-kDa subunit. From a *Haliotis* cDNA library, we have isolated and sequenced a cDNA clone which encodes the five C-terminal FUs d, e, f, g and h of HtH2. As shown by multiple sequence alignments, defg of HtH2 correspond structurally to defg from *Octopus dofleini* hemocyanin. HtH2-e is the first FU of a gastropod hemocyanin to be sequenced. The new *Haliotis* hemocyanin sequences are compared to their counterparts in *Octopus*, *Helix pomatia* and HtH1 (from the latter, the sequences of FU-f, FU-g and FU-h have recently been determined) and discussed in relation to the recent 2.3 Å X-ray structure of FU-g from *Octopus* hemocyanin and the 15 Å three-dimensional reconstruction of the *Megathura crenulata* hemocyanin didecamer from electron micrographs. This data allows, for the first time, an insight into the evolution of the two functionally different hemocyanin isoforms found in marine gastropods. It appears that they evolved several hundred million years ago within the Prosobranchia, after separation of the latter from the branch leading to the Pulmonata. Moreover, as a structural explanation for the inefficiency of the type 1 hemocyanin to form multidecamers *in vivo*, the additional N-glycosylation sites in HtH1 compared to HtH2 are discussed.

**Keywords:** evolution; Gastropoda; hemocyanin; KLH; Mollusca; primary structure.

In molluscs, the blue, copper-containing respiratory protein hemocyanin has a molecular mass of  $\approx 4$  MDa and multiples thereof. These large molecules occur freely dissolved in the hemolymph of many gastropods and also of chitons, cephalopods and some bivalves. The basic 4-MDa unit is a ring-like decamer consisting in a wall of 35 nm in diameter and 18 nm in height, with an internal collar. In cephalopods, native hemocyanin is present exclusively as symmetrical decamers with a central collar, whereas chiton hemocyanins are asymmetrical decamers with a peripheral collar. In bivalves and gastropods, two asymmetrical decamers are assembled face-to-face with a collar complex at each end. In prosobranch and opisthobranch gastropods, and also in a bivalve, didecamers are often accompanied by tube-like multidecamers of varying length which consist in a didecamer with additional decamers assembled at one or both sides [1,2].

The  $\approx 400$ -kDa subunit of mollusc hemocyanins is a polypeptide folded like a pearl chain into seven or eight

globular substructures, the so-called 'functional domains' or 'functional units' (FUs), termed FU-a to FU-h. All FUs possess a molecular mass of  $\approx 50$  kDa and each carries a binuclear copper active site, but they differ considerably in primary structure and immunological properties [1]. From *Octopus dofleini* hemocyanin, the complete amino acid sequence of the seven-FU subunit is available [3]. Moreover, the X-ray structure of an *Octopus* hemocyanin FU dimer has recently been solved at 2.3 Å resolution [4]. From the more complex gastropod hemocyanins, much data on disassembly, reassembly, and oxygen binding behaviour is available [1] and a 15-Å reconstruction of the didecamer has recently been derived from electron micrographs [5], but the sequence data are rather fragmentary. In recent years we and others have studied the hemocyanins intensively from two closely related marine gastropods, the keyhole limpet *Megathura crenulata* [6–13] and the abalone *Haliotis tuberculata* [14]. In both animals the hemocyanin occurs as two isoforms (KLH1 and KLH2 in *Megathura*, HtH1 and HtH2 in *Haliotis*); KLH1/HtH1 and KLH2/HtH2 are interspecifically related. Keyhole limpet hemocyanin (KLH) is a widely used immune stimulator [9,11,12].

From hemocyanin-producing pore cells in the mantle connective tissue of *Haliotis* [15] we have purified mRNA and constructed a cDNA library. By antibody screening, we recently isolated a cDNA clone encoding FU-f to FU-h of HtH1; moreover, the subunit organization of HtH1 has been presented [14]. Here we report complementary experiments with HtH2 which go a considerable step beyond the information available for HtH1: for HtH2, in addition to the three C-terminal FUs, the sequence of FU-d and FU-e has also been determined.

Correspondence to J. Markl, Institut für Zoologie, Universität Mainz, D-55099 Mainz, Germany. Fax: + 49 6131 394652, Tel.: + 49 6131 392314, E-mail: JMarkl@uzomai.biologie.uni-mainz.de  
Abbreviations: FU, functional units; HpH, *Helix pomatia* hemocyanin; HtH, *Haliotis tuberculata* hemocyanin; KLH, keyhole limpet (*Megathura crenulata*) hemocyanin; OdH, *Octopus dofleini* hemocyanin; RtH, *Rapana thomasiana* hemocyanin; SoH, *Sepia officinalis* hemocyanin.

Enzymes: *Staphylococcus aureus* V8 protease type XVII (EC 3.4.21.19); bovine pancreatic elastase type IV (EC 3.4.21.36); bovine pancreatic  $\alpha$ -chymotrypsin (EC 3.4.21.1); bovine pancreatic trypsin type XIII (EC 3.4.21.4).  
(Received 11 May 1999, revised 2 July 1999, accepted 5 July 1999)

## MATERIALS AND METHODS

### Purification of HtH2

Maintenance of animals, hemolymph collection, and isolation of total haemocyanin was essentially as described previously [14]. HtH2, which is the minor haemocyanin component in *H. tuberculata* hemolymph, was purified from HtH1 by anion exchange chromatography using a Mono-Q column on a HPLC apparatus (Applied Biosystems); elution was performed using a NaCl step gradient. Re-chromatography was required to obtain an electrophoretically almost pure HtH2 fraction. Dissociation of HtH2 oligomers into subunits was achieved by overnight dialysis against 0.5 M glycine/NaOH buffer (pH 9.6) at 4 °C.

### Electron microscopy

Conventional negative staining was performed by the single droplet procedure [16] as described elsewhere [14]. A Zeiss EM 900 transmission electron microscope was used for this study.

### PAGE and immunoelectrophoresis

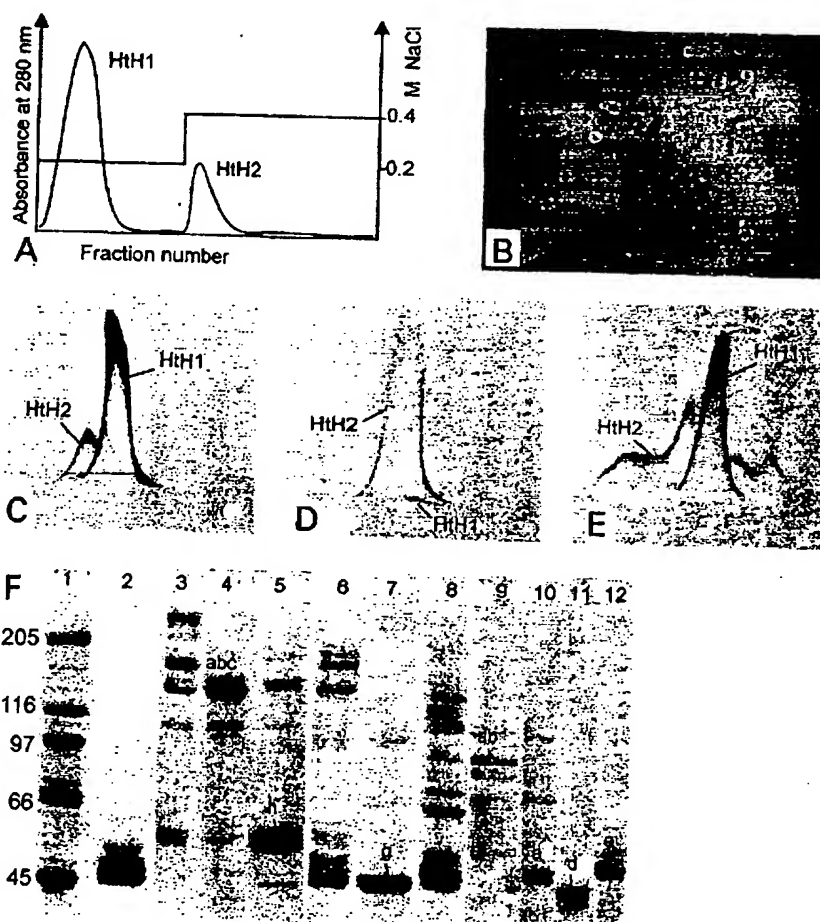
SDS/PAGE was performed according to Laemmli [17]. For native PAGE, an alkaline system according to Markl *et al.* [18]

was used, with 0.33 M Tris/borate (pH 9.6) gel buffer, and 0.065 M Tris/borate (pH 9.6) electrode buffer. Crossed, and crossed-line immunoelectrophoresis were performed as described previously [19,20]. Rabbit antibodies were raised against dissociated total HtH (i.e. HtH1 + HtH2) and purified HtH2 by Charles River Deutschland (Kisslegg, Germany). The immunization procedure was as described by Markl and Winter [21].

### Limited proteolysis and isolation of fragments

Limited proteolysis was performed at 37 °C in 0.13 M glycine/NaOH pH 9.6, by adding one of the following enzymes (Sigma) dissolved in 0.1 M  $\text{NH}_4\text{HCO}_3$  (pH 8.0): *Staphylococcus aureus* V8 protease type XVII (8400), bovine pancreatic elastase type IV (E-0258), bovine pancreatic  $\alpha$ -chymotrypsin (C-3142), bovine pancreatic trypsin type XIII (T-8642). The haemocyanin concentration was between 1 and 10  $\text{mg}\cdot\text{mL}^{-1}$ , and the concentration of the enzyme was 2% (w/w). Proteolysis was terminated after 5 h by freezing at -20 °C. HPLC was performed on an apparatus from Applied Biosystems equipped with a model 1000S diode array detector. Proteolytic fragments were applied to a Mono-Q anion exchange column (Pharmacia) equilibrated with 0.02 M Tris/HCl (pH 8.0) and eluted by a linear NaCl gradient (0–0.5 M) in the same buffer, at a flow rate

**Fig. 1. Purification and characterization of HtH2.** (A) Partial separation of HtH1 and HtH2 from total HtH (resuspended ultracentrifugation pellet) by anion exchange HPLC on a Mono-Q column, using a NaCl step gradient for elution. The first elution peak contained pure HtH1; the second peak contained mostly HtH2, which was still contaminated with HtH1. By re-chromatography of the second peak (data not shown), the remaining HtH1 could almost quantitatively be removed. (B) Electron microscopy of negatively stained HtH2, showing mostly didecamers but also short multidecamers (i.e. tridecamers); bar = 100 nm (C–E) Immunoelectrophoresis using rabbit anti-HtH antibodies. Prior to these experiments, HtH1 and HtH2 were dissociated into subunits. In the first dimension, the anode was on the left (C) Crossed immunoelectrophoresis of total HtH as applied to the experiment shown in (A); anti-HtH1 + HtH2 antibodies from a rabbit were used. In the first dimension, the anode was on the left. (D) Crossed immunoelectrophoresis of HtH2 obtained after re-chromatography; the same antibodies as in (C) were used. (E) Crossed-line immunoelectrophoresis of total HtH, with purified HtH2 in the line to demonstrate which precipitation peak has been obtained; the same antibodies as in (C) were used. (F) SDS/PAGE (7.5% polyacrylamide) of HtH2 proteolytic fragments; the anode was at the bottom. Lanes: 1, molecular weight markers (masses indicated); 2, total cleavage products of subunit HtH2 with elastase; 3, total cleavage products of subunit HtH2 with V8 protease; 6, total cleavage products of subunit HtH2 with trypsin; 8, total cleavage products of subunit HtH2 with chymotrypsin; 4, 5, 7, 9–12, various fragments enriched by HPLC (Fig. 2) and identified as described in the text and shown in Fig. 3.



of  $1 \text{ mL} \cdot \text{min}^{-1}$ . Alternatively, proteolytic fragments were isolated by excising bands from native PAGE gels [18] after inverse staining with the Roti-White system (Roth, Karlsruhe, Germany) as described by Fernandez-Patron *et al.* [22]. For subsequent cleavage with a second enzyme, isolated fragments were first dialysed overnight against  $0.13 \text{ M}$  glycine/NaOH, pH 9.6 to remove the NaCl.

#### Amino acid sequence analysis

Proteins from HPLC were denatured in SDS-containing sample buffer and separated by SDS/PAGE [17]; 7.5% polyacrylamide. To avoid N-terminal blockage, 0.6% (v/v) thioglycolic acid was added to the cathodic buffer [23]. Protein bands were electro-transferred to ProBlot membranes (Applied Biosystems) [12]. Detection of individual polypeptides on the membranes was performed by Ponceau S staining. Polypeptide bands of

interest were cut out and sequenced in a 477A protein sequencer apparatus from Applied Biosystems by H. Heid (DKFZ, Heidelberg, Germany). The quantity of polypeptide applied to the sequencer was in the lower pmol range.

#### cDNA cloning and sequence analysis

A lambda cDNA expression library constructed from poly(A<sup>+</sup>) RNA of *Halotis* mantle tissue using vector lambda ZAP Express<sup>TM</sup> according to the instructions of the supplier (Stratagene) was available in our laboratory [14]. Clones were isolated using a digoxigenin-labelled cDNA probe of 580 bp length corresponding to the C-terminal region of HtH1-g and the N-terminal region of HtH1-h (for sequence analysis of cDNA coding for HtH1, see [14]). cDNA sequencing was performed by commercial services on both strands using the Taq Dye deoxy Terminator system. Sequence alignment was performed with the CLUSTAL W (1.7) and TREEVIEW software packages [24,25].

## RESULTS

#### Isolation of HtH2, and analysis of its subunit organization

Separation of HtH1 and HtH2 by anion exchange chromatography is shown in Fig. 1A. If the HtH2 fractions still contained some HtH1, this impurity was removed by re-chromatography. When examined by electron microscopy, purified HtH2 appeared mostly as didecamers, but the occasional tridecamer was also present (Fig. 1B). This contrasts with HtH1 which consists exclusively of didecamers [14]. Purification of the HtH2 subunit was monitored by dissociation of each chromatographic fraction, at alkaline pH, into subunits followed by crossed, and crossed-line immunoelectrophoresis using anti-HtH1 + HtH2 antibodies raised in a rabbit (Fig. 1C–E). Compared to the starting material shown in Fig. 1C, after the chromatographic purification procedure only a trace of HtH1 was left as a contaminant (Fig. 1D). Crossed-line immunoelectrophoresis of total HtH subunits in the starting hole with the chromatographically isolated subunit material (Fig. 1D) in the line

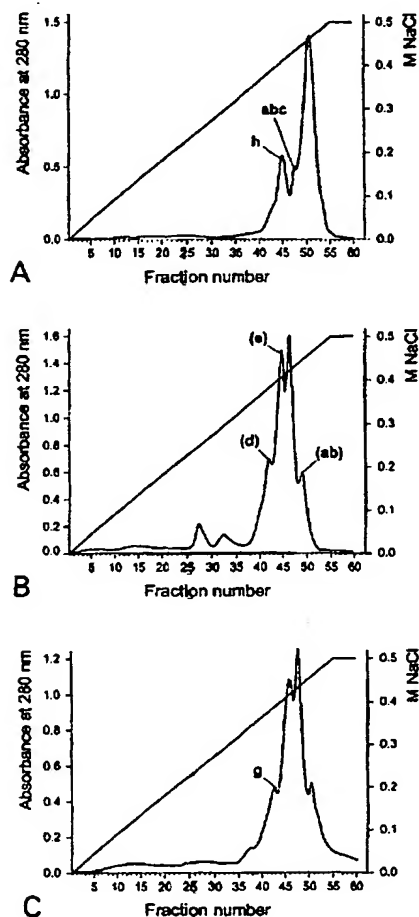
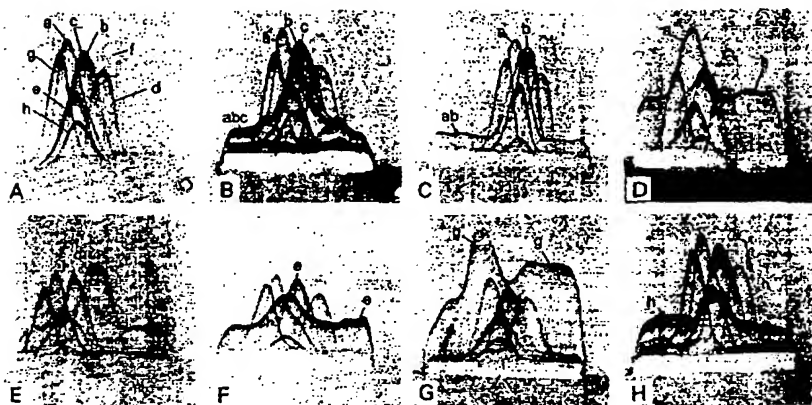


Fig. 2. Separation of proteolytic cleavage products of subunit HtH2 by HPLC. The products of limited cleavage with V8 protease (A), chymotrypsin (B), and trypsin (C) were applied to a Mono-Q column and eluted by a linear NaCl gradient. Components in the fractions were identified by SDS/PAGE (Fig. 1F) and crossed-line immunoelectrophoresis (Fig. 3) as described in the text. Those elution peaks from which a component was used in the final analysis are indicated by labelled arrows. Labels without a bracket indicate that the component was sufficiently pure to be analysed directly. Labels in brackets indicate that further purification by native PAGE was required.

Table 1. N-terminal sequence of isolated FU fragments of HtH and KLH. For more data on KLH1, KLH2 and HtH1, see [9,12,14]. The respective position in the solved primary structure of HtH2-defgh is indicated by position numbers (for HtH2-d and HtH2-e, see Fig. 4; for HtH2-g, see Fig. 5; for HtH2-h, see Fig. 6). Note that in HtH2-e, cleavage by chymotrypsin of an Arg-Pro bond is not very probable; according to Fig. 4, one would expect the sequence <sup>4</sup>LRPD. However, for unknown reasons, the enzyme also removed <sup>4</sup>LR<sup>5</sup> from HtH2-e. In the case of HtH2-g, tryptic cleavage between FU-f and FU-g is more likely at the <sup>416</sup>Arg-Ala bond; however, the expected N-terminal sequence <sup>417</sup>AADSAHS<sup>422</sup> (Fig. 5) was apparently removed from HtH2-g by additional cleavage at <sup>422</sup>Ser-Ala.

Functional unit	N-terminal sequence	Protease used
HtH1-a	DNVVRKDVSHLTDDEVQ	–
KLH1-a	ENLVRKDVERL	–
KLH2-a	VDTVVRKNVDSL	–
HtH2-a	SVDTVLxKNVDNLxD	–
HtH2-d	<sup>6</sup> DEVVTAASHI <sup>15</sup>	Chymotrypsin
HtH2-e	<sup>6</sup> PDGHSDDI <sup>13</sup>	Chymotrypsin
HtH2-g	<sup>423</sup> ANIAGSGV <sup>430</sup>	Trypsin
HtH2-h	<sup>5</sup> VTRQxTDGNA <sup>14</sup>	V8 protease

Fig. 3. Analysis of the subunit organization of HtH2. For immunoelectrophoresis, anti-HtH2 antibodies raised in a rabbit were used throughout; in the first dimension, the anode was on the left. (A) Crossed immunoelectrophoresis showing a panel of eight different FUs as obtained by limited elastase proteolysis of purified subunit HtH2. Identification of the various peaks as HtH2-a to HtH2-h was the net result of a large number of experiments as described in the text and below. (B–H) Crossed line immunoelectrophoresis of elastase-cleaved subunit HtH2 as shown in (A), with HPLC-isolated proteolytic fragments of subunit HtH2 in the line to identify to which precipitation peak(s) they correspond (for HPLC profiles, see Fig. 2; for SDS/PAGE of fragments, Fig. 1F). Identification of the fragments was achieved by N-terminal sequencing (Table 1).



demonstrated that the bulk protein was indeed HtH2 (Fig. 1E). N-terminal sequencing of the HtH2 subunit revealed a single primary structure which confirmed that this material was sufficiently homogeneous for further analysis; the sequence obtained showed similarity to FU-a from HtH1, KLH1 and notably KLH2 (Table 1).

The seven or eight functional units (FUs) constituting a molluscan haemocyanin subunit usually lack immunological cross-reactivity as deduced from crossed immunoelectrophoresis, and this observation is in accord with the considerable difference in primary structures [9,12,26,27]. With isolated HtH2 subunit (Fig. 1D), we used low concentrations of four different proteases (elastase, V8 protease, trypsin, and chymotrypsin), which in HtH1, KLH1 and KLH2 had cleaved the

exposed polypeptide chain between neighbouring FUs, without destroying peptide bonds within the FUs [9,12,14]. The cleavage products were studied by SDS/PAGE (Fig. 1F). Elastase produced mostly fragments migrating on SDS/PAGE close to 50 kDa, which corresponds to single FUs (Fig. 1F, lane 2). The other three enzymes also yielded some ~50-kDa products, but in addition produced FU dimers, trimers and larger fragments of the HtH2 subunit (Fig. 1F, lanes 3, 6 and 8).

HPLC (Mono-Q) separation of the V8 protease cleavage products of subunit HtH2 yielded two fused elution peaks (Fig. 2A). In a fraction at the leading edge of the second peak, a fragment of ~150 kDa was highly enriched (Fig. 1F, lane 4). This component was purified by blotting, sequenced and exhibited the same N-terminal sequence as the intact subunit

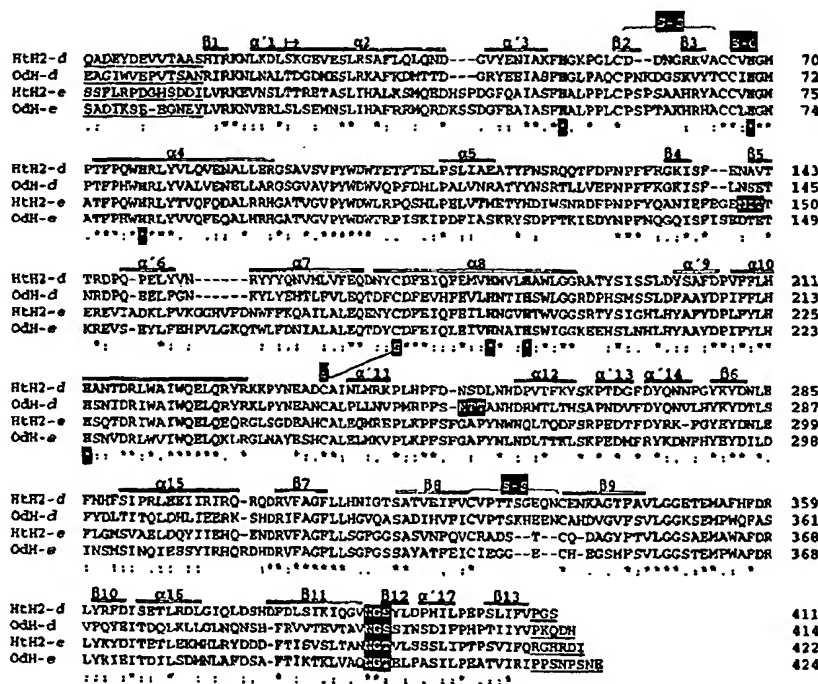


Fig. 4. Multiple sequence alignment of FU-d and FU-e from HtH2 and *Octopus* haemocyanin. The linker regions between neighbouring FUs are underlined. On the top of each sequence block the secondary structure elements of OdH-g according to Miller *et al.* [3] are indicated; for their position in the X-ray structure [4], see Fig. 7. Strictly conserved residues are marked by an asterisk (identical); isofunctional exchanges are marked by either a colon (very similar) or by a point (similar). Copper ligand histidines are marked by reversed asterisks. Potential disulfide bridges and N-glycosylation sites are indicated by black boxes. The alignment was performed with the CLUSTAL software. The OdH sequences are taken from Miller *et al.* [3].

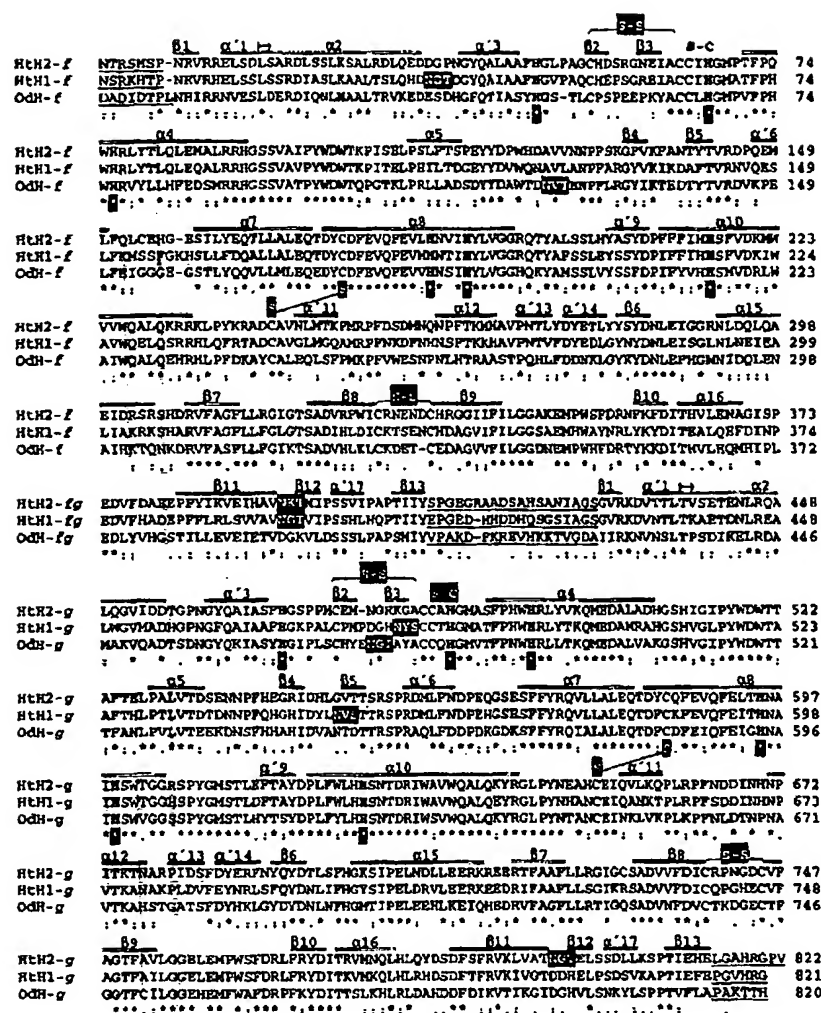


Fig. 5. Multiple sequence alignment of FU-fg from HtH2, HtH1 and *Octopus haemocyanin*. Codes are the same as those used in Fig. 4. The HtH1 sequences are from Keller *et al.* [14]; the OdH sequences are from Miller *et al.* [3].

(Table 1) and therefore represented HtH2-abc. Crossed immunoelectrophoresis of the elastase cleavage products of subunit HtH2 showed eight discrete immuno-precipitation peaks (Fig. 3A), which on correlation with the results from SDS/PAGE (Fig. 1F, lane 2) represent the individual FUs. In crossed-line immunoelectrophoresis, HtH2-abc fused completely with three of the eight immunoprecipitation peaks of the elastase cleavage pattern (Fig. 3B).

HPLC separation after chymotryptic cleavage of the intact subunit yielded several fused elution peaks (Fig. 2B). The last peak almost exclusively contained a fragment of  $\approx 100$  kDa (Fig. 1F, lane 9), which showed the same N-terminal sequence as HtH2-abc (Table 1) and therefore represented HtH2-ab. Crossed-line immunoelectrophoresis of this HPLC fraction revealed a single protein, which completely fused with two FUs from the elastase cleavage pattern (Fig. 3C). Both are also part of HtH2-abc (Fig. 3B), and therefore must represent HtH2-a and HtH2-b. This, by deduction, identified the third component incorporated in HtH2-abc as FU-c (Fig. 3B). Isolated HtH2-ab (Fig. 1F, lane 9) was cleaved by elastase, resulting in several products; the major protein could be isolated by excising its band from a native PAGE gel. In SDS/PAGE, it showed a

molecular mass of  $\approx 50$  kDa (Fig. 1F, lane 10), and its N-terminal sequence identified this FU as HtH2-a (Table 1). The precipitation peak of HtH2-a was revealed by crossed-line immunoelectrophoresis (Fig. 3D); thus, the still remaining component of HtH2-abc must be HtH2-b (Fig. 3B). At this stage of the analysis, FU-a, FU-b and FU-c were identified in the pattern of crossed immunoelectrophoresis (Fig. 3A).

A fragment of  $\approx 45$  kDa found in the first HPLC elution peak after chymotryptic cleavage (Fig. 2B) was further enriched by excising its band from a native PAGE gel. After this procedure, the eluted protein showed a satisfactory purity in SDS/PAGE (Fig. 1F, lane 11). Similarly, from the second HPLC peak of the chymotryptic cleavage products a 55-kDa fragment was obtained (Figs 2B and 1F, lane 12). Both fragments were N-terminally sequenced (Table 1), and then identified as HtH2-d and HtH2-e by aligning their sequences to the primary structure derived from a cDNA coding for HtH2-defgh (see below). Subsequently, they were assigned to their respective immunoprecipitation peak in the elastase cleavage pattern of subunit HtH2 by crossed-line immunoelectrophoresis (Fig. 3E,F). As a consequence, five of the eight FU precipitates were now identified (Fig. 3A).

HtH2-h	E T E V T R Q H T D G N A H - F H R K E V D S L S D E A N N L K N A L Y K L O N D H S L T Q Y E A I S G Y N C T P N L C P E E G D D K I P C C V E	74
HtH1-h	K H E D - E H D D R L A D V L T R K E V D P L S L Q E A N A I K D A L Y K L O N D S K G G P E A I A G Y E G Y P N C P E R C T Q Y P C C V E	74
HtH2-h	G N O I P P Y W R L L T I Q L E R A L E N G A L L G V P Y W D N K D L S L P A F T S D S S N N P Y F K Y H I A G V G H D T V R E P T S L T Y	149
HtH1-h	C M P V P P H W R L H T I Q M E R A L O N G S P H G I P Y W D T Q O M S L P S F P G D S S N N P F K Y I R C V G H E T T R D V N Q R L P	149
HtH2-h	N Q P Q I H G Y D Y L Y L A L T L E E N V C D F E V Q Y E I L R N A V S W L G S Q K Y S A S T L E Y S A F D P V P M L S G L D R L M T I	224
HtH1-h	E E P Q E F D Y L Y L T L Q V L E R S Y C D F E V Q Y E I L R N A V S W L G T G Q Y S A S T L E Y S A F D P V P M I H S S L D R I W I L	224
HtH2-h	W Q E L Q R I R R K P Y N P A K C A - Y H M G E R P L A P F S Y P S I M Q D E F T R A N S K P S T V F D Q H K P C T Y I N D L N V R C H S T Q E L M T	298
HtH1-h	W Q L Q R I R R K P Y A L D C A G D R L M K D P L R P N Y E T V N E D E F T R I N S P S I L P D H Y P N Y E V D N H I R C Q D T H E L E R	299
HtH2-h	I I N D L A N T O R I Y A G P V L S G I G T S A S V E I Y L R T - - D D N D E E - V G T F T V L G C E R E M P W A Y E R V F K Y D I T E V A D R L K L	370
HtH1-h	V I Q E L R N K D R I F A G P V L S G L R I S A T V K V F I H S K E D S H E E Y A G E F A V L G G E K E M P A Y E R L K L D I S D A V H K L H V	374
HtH2-h	S Y G D T F N F L E I T S Y D G S V V S G L F N F P I I Y R P A N H D Y D V L V E P T Q R N L H I P P K V V K C T R I E F H P V D D S V R P	445
HtH1-h	K D E D I R - F R V V V T A Y N G D V T T R L S Q F F I V H R P A H V A D I L V E P T Q A G H L P P K V V K S G T K V E P T D S S V N K A	448
HtH2-h	V V D L G S Y T A L P K C V P P P T H C P E L A N H V S V K P G D Y Y V T G P T A D L C Q N A D V R I H I K V E D S	505
HtH1-h	M V E L G S Y T A N A K C I V P P F S Y H G F E L D K V S V D H G D Y Y I A A G T H A L C E - Q N L R L H T K V E E S	507

Fig. 6. Sequence alignment of FU-h from HtH2 and HtH1. The linker region between FU-g and FU-h is underlined, the start motif of the unique C-terminal extension of FU-h is also underlined and marked by bold letters. Codes are the same as those used in Fig. 4. Note that compared to other FUs, the third disulfide bridge is missing in both FU-h versions. Also note conservation of two cysteines in the C-terminal extension, which probably allow formation of an additional disulfide bridge. #, C-terminus of polypeptide chain. The HtH1 sequence is from Keller *et al.* [14].

HPLC separation after tryptic cleavage of the intact HtH2 subunit yielded four fused elution peaks (Fig. 2C). In SDS/PAGE, the first peak showed a strong protein band of  $\approx 45$  kDa (Fig. 1F, lane 7). By N-terminal sequencing and alignment to the sequence of HtH2-defgh it was identified as HtH2-g (Table 1). This FU fused, in crossed-line

immunoelectrophoresis, with one of the three remaining peaks of the elastase cleavage pattern (Fig. 3G), which was thereby identified, in the total pattern, as HtH2-g (Fig. 3A). The first HPLC peak of the V8 protease cleavage products of subunit HtH2 (Fig. 2A) contained almost exclusively a  $\approx 60$  kDa fragment (Fig. 1F, lane 5). It fused, in crossed-line immunoelectrophoresis, with one of the two yet unidentified FU precipitates of the elastase cleavage pattern (Fig. 3H). According to its N-terminal sequence in comparison to the primary structure of HtH2-defgh, this component was identified as HtH2-h (Table 1). After this approach, there was just a single precipitate left which could not be isolated but in all probability represents FU-f; consequently, the entire FU organization of the HtH2 subunit was deciphered (Fig. 3A).

#### Sequencing of a cDNA clone encoding five functional units of HtH2

A cDNA expression library constructed from *H. tuberculata* mantle tissue was screened using a cDNA probe encoding a region of HtH1-gh (see Methods). Cross-hybridization of this probe resulted in isolation and sequence analysis of several new cDNA clones of varying length which all encoded the C-terminal region of the same haemocyanin polypeptide; it was clearly different from HtH1. The largest of these cDNA clones contained 6726 bp. The cDNA sequence is not shown here, but is available in the EMBL data bank (accession number AJ012048). This clone, termed *hth2-defgh*, contains an open reading frame for a polypeptide of 2160 amino acids (Figs 4–6) with a calculated molecular mass of 248 kDa. The translated region must represent the C-terminal part of the polypeptide and not a random fragment, because the open reading frame is terminated by a stop codon followed by a untranslated region of 243 bp with a polyA tail. Alignment with other molluscan haemocyanin sequences, notably from *Octopus* haemocyanin [3] and HtH1 [14] revealed that the encoded polypeptide encompass five complete FUs, and comparison to the N-terminal sequences shown in Table 1 identified it as part of HtH2. It starts in the linker region between HtH2-c and HtH2-d and contains the complete amino acid sequence of HtH2-d, HtH2-e, HtH2-f, HtH2-g and HtH2-h (Figs 4–6). From our

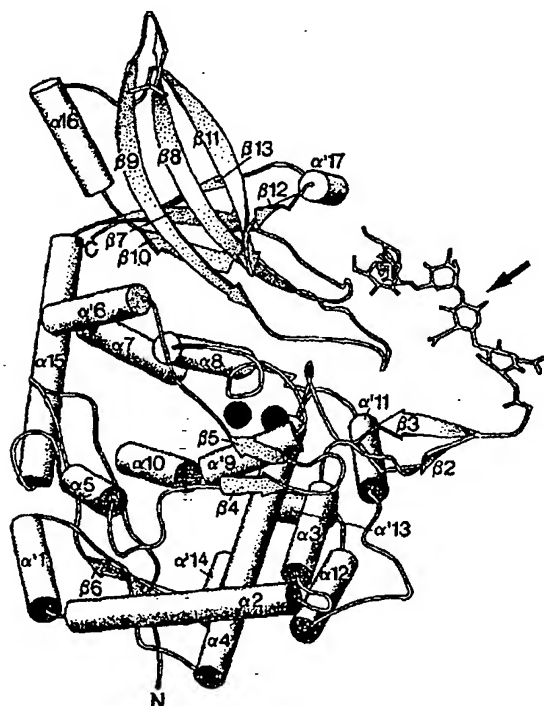


Fig. 7. Schematic view of the X-ray structure of OdH-g, showing positions of the secondary structure elements indicated in Figs 4–6. Arrow, asparagine-linked carbohydrate side chain (molecular mass  $\approx 1000$  Da). Drawn from Miller *et al.* [3] and Cuff *et al.* [4].



		% Similarity																	
FU		HtH1-f	HtH2-g	HpHβ-g	OdH-g	SoH[h]-g	RtH2-a	HtH2-d	OdH-e	OdH-b	OdH-c	HtH1-f	HtH2-f	OdH-f	OdH-d	HtH2-d	HpHβ-d	OdH-d	HtH1-h
HtH1-f	26	100	63	59	58	52	49	43	46	47	42	47	45	45	45	47	46	42	41
HtH2-g	37	35	100	54	54	57	47	46	46	43	45	44	44	44	44	46	45	40	42
HpHβ-g	41	43	46	100	75	51	47	42	44	44	41	46	45	43	45	45	42	40	40
OdH-g	42	44	46	24	100	51	46	44	44	43	41	46	45	43	45	45	42	40	40
SoH[h]-g	48	48	47	49	49	100	48	46	42	41	44	45	50	43	45	52	39	41	42
RtH2-a	51	53	53	53	54	52	100	56	48	42	47	45	45	41	45	46	42	40	42
HtH2-d	57	57	54	58	56	54	44	100	45	41	44	43	41	40	44	45	44	38	38
OdH-e	54	56	54	54	56	58	52	35	100	45	43	43	43	44	43	43	43	38	38
OdH-b	53	53	54	56	57	59	54	39	33	100	42	43	42	41	40	42	43	38	40
OdH-c	57	55	57	58	59	56	53	36	33	58	100	44	43	43	43	43	47	41	39
HtH1-f	57	55	57	58	59	56	53	36	33	58	44	100	43	43	43	43	47	41	39
HtH2-f	53	52	53	54	55	55	53	37	33	57	56	49	100	45	45	45	48	41	41
OdH-f	53	58	56	55	55	50	53	39	37	58	49	51	43	100	43	44	44	39	39
OdH-d	53	57	56	56	57	57	59	60	56	59	57	53	57	60	100	42	42	42	42
HtH2-d	53	55	56	55	55	55	54	57	57	57	55	56	54	56	54	100	43	40	41
HpHβ-d	54	53	54	55	55	48	54	55	57	57	57	55	56	58	56	48	100	47	47
OdH-d	53	54	53	58	58	61	59	56	57	57	53	52	58	61	64	58	60	100	60
HtH1-h	58	58	60	61	60	60	62	62	62	59	59	61	64	61	64	58	59	61	100
HtH2-h	57	59	58	58	60	58	58	62	62	60	61	59	61	63	58	59	61	60	60

Fig. 8. Matrix of percentage similarity (top) and percentage diversity (bottom) in compared sequences from molluscan haemocyanin FUs. Multiple sequence alignment was performed with the CLUSTAL software. The sequences are derived from haemocyanin of the prosobranch gastropods *H. tuberculata* (HtH) and *Rapana thomasiana* (RtH), the pulmonate gastropod *Helix pomatia* (HpHβ), and the two cephalopods *O. dofleini* (OdH) and *Sepia officinalis* (SoH). For sources, see [3,14,29,30,40].

analysis of the FU organization of the HtH2 subunit (see above) as well as from the absence of a start codon and a sequence coding for a signal peptide, we are sure that clone *htH2-defgh* does not encode the entire haemocyanin polypeptide and that the three N-terminal FUs are still missing. A multiple sequence alignment of HtH2-d, HtH2-e and the corresponding FUs in *Octopus dofleini* haemocyanin [3] is presented in Fig. 4. In Fig. 5 a multiple alignment of HtH2-fg with HtH1-fg [14] and OdH-fg [3] is shown. In Fig. 6 we compare the sequences of HtH2-h and HtH1-h [14]. For clarification, Fig. 7 shows the published X-ray structure of OdH-g [4]. Figure 8 shows the

structural similarities and diversities calculated from a multiple alignment which includes the 19 complete sequences of molluscan haemocyanin FUs currently available, and Fig. 9 presents the unrooted, radial representation of a phylogenetic tree constructed from the same alignment.

## DISCUSSION

### The HtH2 subunit is segmented into eight different functional units

Our data show the existence of eight different FUs in HtH2, and reveal their sequential arrangement within the elongated subunit (Fig. 3A). Implications of such analyses are discussed in detail elsewhere [9,12,14], but it is clear that understanding the FU organization is a prerequisite for all future structural studies on a particular haemocyanin. With respect to HtH2, it should be pointed out that in this case, for the first time, such an analysis was accompanied directly by cDNA sequencing which greatly helped to decipher the FU arrangement. Although the HtH2 pattern differs, in electrophoretic details, from all other molluscan haemocyanin FU panels analysed so far (which are different internally and also from each other, e.g. [9,12,14,26,27]), the presence of eight different FUs has clearly emerged as being broadly applicable to gastropod haemocyanins. This has now also been established for the subunits of KLH2 and RtH2, which have previously been proposed to contain, respectively, seven [9] and five [28] different FUs; more recently both have been shown to possess eight FUs (W. Gebauer *et al.* unpublished data). Moreover, it is evident that FU-h is an additional FU type found only in gastropods, bearing in mind that *Sepia* FU-'h' is known to correspond to *Octopus* FU-g [1]; this FU is therefore termed here SoH[h]-g, as proposed recently [14].

### Functional units HtH2-d and HtH2-e

FU-d from the pulmonate gastropod *Helix pomatia* was the first molluscan haemocyanin polypeptide to be sequenced [29] and it has been repeatedly compared in detail to the more recently obtained FU primary structures, notably from *Octopus* haemocyanin [3]. However, this early sequence may still contain errors, although some corrections have recently been published [30]. Therefore, in the present alignment, we concentrate on comparing the primary structures of *Haliotis* and *Octopus* haemocyanin (Fig. 4), both of which have been deduced entirely from their cDNA sequences. The primary structure of HtH2-e

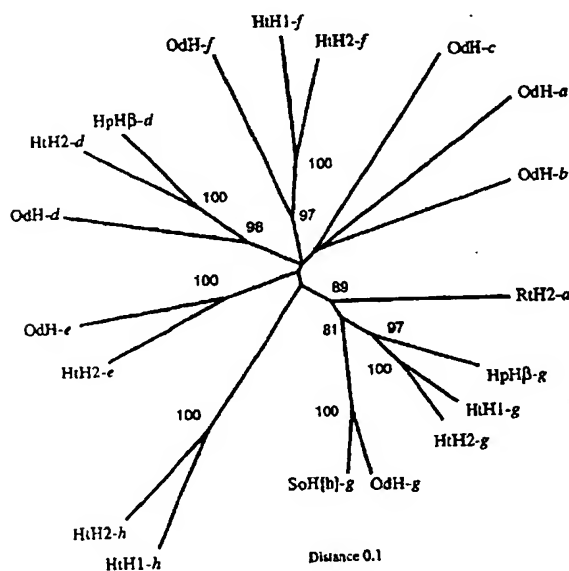


Fig. 9. Radial phylogenetic tree of molluscan haemocyanin FUs. This unrooted tree is based on a CLUSTAL multiple alignment of the currently available sequences (for sources, see [3,14,29,30,40]). For abbreviations see Fig. 8. Bootstrap percentages are based on 1000 replicates. Only bootstrap values > 50 are shown. Note that with the exception of RtH2-a, topologically corresponding FU types group as a common branch. Assuming that the branching node of gastropod and cephalopod haemocyanin lies 520 million years ago, the common origin of the eight FU types dates back ≈ 650 million years, and the branching node of HtH1 and HtH2 lies ≈ 300 million years ago.

derived from cDNA clone *hth2-defgh* is the first complete sequence of a gastropod haemocyanin functional unit of type e. The only other available sequence of this FU type comes from *Octopus* haemocyanin (Fig. 4).

Alignment of the FU-d and FU-e protein sequences from HtH2 and OdH shows a structural similarity of 52% for HtH2-d/OdH-d and 56% for HtH2-e/OdH-e, whereas comparison of FU-d to FU-e gives a significantly lower score of 42% and 44%, respectively (Fig. 8). This type-specific structural similarity is also evident from the four deletions/insertions by which FU-d differs from FU-e (Fig. 4). An alignment of all available molluscan haemocyanin sequences revealed that the gaps in FU-d, which in HtH2 are defined by <sup>41</sup>HSP<sup>43</sup> and <sup>163</sup>GGHVFDN<sup>169</sup>, are caused by specific deletions in FU-d, whereas <sup>144</sup>EG<sup>145</sup> is an insertion in FU-e (shared by OdH-b [3]). The fourth variable motif, defined in HtH2-d by <sup>332</sup>SQEQCEN<sup>339</sup>, seems to be rather susceptible to insertion/deletion events as deduced from the seven *Octopus* FU sequences [3], but also in this case, conservation of sequences specific for FU-d on the one hand and FU-e on the other is impressive (Fig. 4). It should be noted that all of these insertions/deletions occur at positions which correspond, in the X-ray structure of OdH-g [4], to irregularly structured regions between  $\alpha$ -helices or  $\beta$ -sheets (indicated in Fig. 4 and shown in Fig. 7).

Except for occasional amino acids, HtH2-d and OdH-d differ only in a few short motifs, for example <sup>121</sup>QQT<sup>123</sup> versus <sup>121</sup>TLL<sup>123</sup> (Fig. 4); however, they are also located between secondary structure elements [4]. Interestingly, the motif <sup>357</sup>FDR<sup>359</sup> which Miller *et al.* [3] found in five of the seven *Octopus* haemocyanin FUs but not in OdH-d, is present in HtH2-d (Fig. 4). The only somewhat variable sequence of FU-d within a secondary structure element is <sup>382</sup>DLSI<sup>385</sup> versus <sup>382</sup>RVVT<sup>385</sup> (strand  $\beta$ 11), but even in this case, one hydrophobic residue has been conserved. Thus, FU-d from *Octopus* and *Haliois* are very similar structurally (with the exception of possible carbohydrates; see below), and there is little doubt that they represent corresponding structural and functional elements within their respective native haemocyanin oligomers.

There are only a few regions in which HtH2-e differs considerably from OdH-e, notably the sequence motifs <sup>119</sup>TWSNRDF<sup>125</sup>, <sup>163</sup>GGHVFDN<sup>169</sup> and <sup>342</sup>RADST<sup>346</sup>. However, as deduced from the X-ray structure of OdH-g (Figs 4 and 7), all three motifs are located in loops connecting secondary structure elements. A fourth region of considerable variability is the tail <sup>414</sup>FQRGHR<sup>420</sup> which, however, is part of the presumably exposed linker region between HtH2-e and HtH2-f. On the other hand, there are several motifs which are identical in both FU-e versions and different in all other sequenced FUs, for example <sup>265</sup>SFGAP<sup>269</sup>. And ultimately, HtH2-e and OdH-e have exactly the same number of amino acids (420). All of these structural features, together with the overall similarity of the two sequences and the strictly conserved insertions/deletions, clearly suggest that in the architecture of their respective haemocyanin, HtH2-e and OdH-e play a very similar structural and functional role.

An obvious difference between HtH2-de and OdH-de concerns potential asparagine-linked carbohydrate attachment sites. FU-d and FU-e from both species possess such a site in exactly the same position close to the C-terminus (Fig. 4), where in OdH-g the loop between strands  $\beta$ 11 and  $\beta$ 12 is localized (Fig. 7). However, in OdH-d but not in HtH2-d an additional site for N-glycosides exists, at a position which corresponds, in the X-ray structure of OdH-g, to the loop between between  $\alpha$ '11 and  $\alpha$ '12 (Figs 4 and 7). The other way

round, HtH2-e possesses a second site for N-glycosides (between strands  $\beta$ 4 and  $\beta$ 5) which is absent in OdH-e (Fig. 4). In this context it should be noted that the amount of carbohydrate side chains per FU varies considerably among the molluscan haemocyanin FUs sequenced so far, with up to three potential sites and an unexpected variety of monoantennary and diantennary side chains detected in *Helix pomatia* (see [3,31]).

#### Functional units HtH2-f, HtH2-g, and HtH2-h

The existence of two very different haemocyanin isoforms in some marine gastropods was first indicated in 1981 [32], and later, many structural and functional differences have been revealed [6,9–14,33,34], but this is the first opportunity to compare them at the level of their primary structures. The structural similarity of FU-fgh from both HtH1 and HtH2 is striking (Figs 5 and 6); it is 64% for FU-f, 74% for FU-g, and 60% for FU-h (Fig. 8). Only the linker regions between neighbouring FUs and several loops connecting  $\alpha$ -helices or  $\beta$ -sheets show considerable variability, for example between  $\alpha$ '6 and  $\alpha$ '7 (Fig. 5) or between  $\alpha$ '10 and  $\alpha$ '11 (Fig. 6).

Compared to the corresponding sequences in *Octopus* haemocyanin, structural conservation is 49–51% for FU-f and 57–59% for FU-g (Fig. 8). Such a degree of invariance between gastropod and cephalopod haemocyanin could probably be expected for the six 'wall forming FUs' (i.e. FU-a to FU-f), which according to current models of the quaternary structure are involved in the cylinder wall of the decamer [1]. However, for FU-g as a 'collar/arc forming FU', it is rather unexpected that its invariance is even higher, because the central collar of cephalopod haemocyanins differs considerably from the peripheral collar/arc complex of gastropod haemocyanins, an observation which has to date prevented construction of a common model of the quaternary structure [1,5,35,36,37]. In *Octopus* haemocyanin decamers, 10 FU-g copies form the central collar [36,37]. This structure seems to correspond, in gastropod haemocyanin decamers, to the arc which lies underneath the peripheral collar [5,35]. On the other hand, it is known that in gastropods, the collar/arc complex is formed by 10 copies of FU-g and FU-h, respectively [1]. From the phylogenetically rather conserved primary structure of FU-g (Fig. 5) it can now be predicted that this FU type fulfils a very similar structural role in cephalopods and gastropods, which would mean that in gastropod haemocyanin decamers it forms the entire arc, leaving FU-h as the only element for the peripheral collar. This is useful information for the major unsolved problem of the molluscan haemocyanin quaternary structure: the exact path and orientation of the multi-FU subunit within the decamer [5,36].

As with HtH1-h [14], HtH2-h also shows the peculiar C-terminal tail of  $\approx$  95 amino acids (Fig. 6), which is absent from other FUs. Characteristics of this polypeptide elongation have been discussed previously for HtH1-h [14]. In the present context it should only be pointed out that even its length is extremely conserved in both HtH isoforms. Provided that this elongation is some kind of anchor to other structural elements, its invariance in both haemocyanins suggests that their peripheral collars are much more similar than proposed previously for the equivalent proteins in *Megathura*, KLH1 and KLH2 [9,12].

#### Potential N-glycosylation sites and possible consequences for assembly

In *Megathura*, KLH2 forms multidecamers; this is not observed with KLH1, at least not *in vivo* (e.g. [6]). Also in *Haliois*, a



portion of native HtH2 is assembled beyond the didecamer (Fig. 1B), whereas native HtH1 is fully restricted to the didecameric state [14]. An interesting aspect in comparing the sequences of HtH1-fgh and HtH2-fgh is therefore to find specific differences which could explain this behaviour, and the most obvious difference is their potential asparagine-linked N-glycosylation sites (sequence motifs NXT and NXS, see Figs 4–6). HtH1-f and HtH2-f both show such a site close to the C-terminus, between strands  $\beta 11$  and  $\beta 12$ , but HtH1-f has an additional N-glycosylation site between helices  $\alpha 2$  and  $\alpha 3$ , which is close to the N-terminus. In HtH1-g there is a site for N-glycosides in the region of the first disulfide bridge as in OdH-g, and another one between strands  $\beta 4$  and  $\beta 5$ , whereas HtH2-g has a single site between strands  $\beta 11$  and  $\beta 12$ . HtH2-h shows a single N-glycosylation site between sheet  $\beta 12$  and helix  $\alpha' 17$ . In contrast in HtH1-h, two rather unusual N-linked carbohydrate sites exist. The first is localized, according to the X-ray structure, between helices  $\alpha' 6$  and  $\alpha 7$ , a region of the core domain where in *Octopus* only FU-c has a site for N-glycosides. The second is totally unique (as far as sequences are available yet) and localized far outside in the so-called 'β-sandwich domain' [4], in a region defined by the loop between strands  $\beta 8$  and  $\beta 9$  (Figs 6 and 7).

A gastropod hemocyanin decamer wall consists of three fenestrated tiers, with the peripheral collar anchored to the upper tier and the internal arc attached to the central tier. In a didecamer, two decamers are assembled 'face-to-face' at their lower tiers. In a tridecamer, an additional decamer is attached, with its lower tier to the upper tier of a didecamer. FU-g appears to be restricted to the arc (see above) and then would be buried too deeply inside the cylinder to interact with a neighbouring decamer. This is different for FU-h, 10 copies of which seem to form the collar, and FU-f which is thought to be involved in the upper tier of the cylinder wall [1,8,35,36]. Thus both FU types could well interact with the lower tier of a neighbouring decamer, and the additional carbohydrate side chains anchored to HtH1-f and/or HtH1-h could probably be involved in blocking multidecamer formation in HtH1, whereas absence of these side chains in HtH2-f and/or HtH2-h would allow such an oligomerization in HtH2. However, this concept is highly speculative, and it does not explain why multidecamer formation in KLH1 from electrophoretically and immunologically intact subunits could be achieved *in vitro* [33,34]. Future deglycosylation experiments under native conditions as well as the sequence analysis of KLH1 and KLH2 should help to substantiate these ideas.

#### Implications for the evolution of molluscan hemocyanin

Of the protostome phyla, the molluscs are among the most ancient and diverse, and molecular data of their hemocyanin might be useful to examine their major divergencies which are still much debated (for example [38,39]). In Fig. 9, an unrooted radial representation of the phylogenetic tree is presented, because so far no outgroup is available; using tyrosinase as the outgroup as suggested by Miller *et al.* [3] was not found to improve the tree, because the relationship of tyrosinase and molluscan hemocyanin is too remote. It has been suggested that the molluscan hemocyanin subunit evolved by three successive duplications of the proto-gene for the functional unit, each followed by gene fusion [1]. However in their phylogenetic analyses, Miller *et al.* [3] found it to be impossible to resolve the evolutionary branching orders among the FUs, indicating that they evolved very rapidly from their ancestral precursor. Indeed, from sequence alignments which include the new HtH2

primary structures it was also not possible to trace these early events, because the branching pattern of the different FU types is highly unstable (Fig. 9). However, reconstruction of the tree with different methods only affected nodes that in the present tree are not bootstrap-supported, but did not influence the conclusions based on the bootstrap-supported branches. In the tree, FU-d, FU-e, FU-f, and FU-g from both molluscan classes form four stable branches (Fig. 9). This confirms that at least these four FU types already existed long before gastropods and cephalopods separated, and that the members of each branch are equivalent in structure and function [1]. The only exception is HtH2-a [40], because its incorporation in the FU-g branch is very stable (Fig. 9). Sequence analysis of FU-a from other gastropod haemocyanins is required to approach this specific problem.

In fossil records, the first gastropods occur in the earliest Cambrian, and the first cephalopods appear somewhat later, about 520 million years ago [41]. This separation event between gastropods and cephalopods might be used to calibrate a molecular clock (for an appropriate formula, see [42]), although the sequence similarities shown in Fig. 8 suggest that this clock may run at different rates among the different FU types. For example, FU-f from HtH1 and HtH2 share 64%, FU-g 74% and FU-h 60% similarity (Fig. 8), and this may well reflect different structural and/or functional constraints influencing the evolution rate of the various FU types. Therefore it is probably too early for a reliable overall calculation to be obtained. Nevertheless, from the distances given in Fig. 8 for FU-g as the most completely analysed FU type, we estimate that the multiple FU subunit originated from a proto-gene about 650 million years ago (for method, see [42]). This fits recent calculations from 22 nuclear genes, which suggest that the major branches of the triploblastic metazoans separated about 830 million years ago, long before the Cambrian explosion, 540 million years ago [42]. In this context it should be considered that the elongated subunit is the prerequisite for oligomerization, and that in turn oligomerization is required for hemocyanin to function as an extracellular blood oxygen carrier [1]; therefore, the multiple FU subunit most probably evolved when triploblastic metazoans reached a level of complexity and activity that required such a carrier protein. According to the estimation above, it took them  $\approx$  180 million years to reach this point, and then another 100 million years to develop forms which could be fossilized. The distance values between HtH1-g/HtH2-g and HpHb-g suggest that separation of prosobranch and pulmonate hemocyanin occurred about 400 million years ago. Indeed, the first fossil pulmonate and opisthobranch gastropods occur in the Carboniferous, some 360 million years ago [41]. According to the distance between HtH1-g and HtH2-g (Fig. 8), separation of their ancestral genes happened about 300 million years ago, either in the late Carboniferous or the early Permian. An outburst of phylogenetic change among the archaeogastropods in the later Paleozoic [41] is probably the background of the evolution of two distinct hemocyanin forms within the same animal.

It should be appreciated that these are very preliminary calculations; the complete hemocyanin subunit sequences from several molluscan classes will be required to obtain more reliable data. A comparative combination of the rapidly increasing knowledge of the primary structure of the two hemocyanin isoforms of *Halioris* with the sequence of *Octopus* haemocyanin [3], the X-ray structure of OdH-g [4], and the 15 Å structure of the KLH1 didecamer [5] is a scientifically meaningful way to approach the remaining questions on the quaternary structure, evolution and function of these intriguing

copper-containing respiratory proteins. Moreover, determination of more molluscan hemocyanin sequences could well assist tracing ancient events in molluscan phylogeny.

## ACKNOWLEDGEMENTS

We thank the Biosyn Company (Fellbach, Germany) and S.M.E.L. (Blainville sur Mer, France) for kindly providing the abalones, H. Heid (DKFZ Heidelberg, Germany) for the N-terminal protein sequence analyses, and J. R. Harris (University of Mainz, Germany) for providing the electron micrographs and critical reading of the manuscript. We also thank H. Storz for excellent technical assistance and K. Rehlinger for the drawing. This work was financially supported by the Biosyn Company and by a grant to J. M. from the Deutsche Forschungsgemeinschaft (Ma 843/4-2).

## REFERENCES

- van Holde, K.E. & Miller, K.I. (1995) Hemocyanins. *Adv. Prot. Chem.* **47**, 1–81.
- Herskovits, T.T. & Hamilton, M.G. (1991) Higher order assemblies of molluscan hemocyanins. *Comp. Biochem. Physiol.* **99B**, 19–34.
- Miller, K.I., Cuff, M.E., Lang, W.F., Varga-Weisz, P., Field, K.G. & van Holde, K.E. (1998) Sequence of the *Octopus dofleini* hemocyanin subunit: structural and evolutionary implications. *J. Mol. Biol.* **278**, 827–842.
- Cuff, M.E., Miller, K.I., van Holde, K.E. & Hendrickson, W.A. (1998) Crystal structure of a functional unit from *Octopus hemocyanin*. *J. Mol. Biol.* **278**, 855–870.
- Orlova, E.V., Dube, P., Harris, J.R., Beckman, E., Zemlin, F., Markl, J. & van Heel, M. (1997) Structure of keyhole limpet hemocyanin type I (KLH1) at 15 Å resolution by electron cryomicroscopy and angular reconstruction. *J. Mol. Biol.* **271**, 417–437.
- Markl, J., Savel-Nieman, A., Wegener-Strake, A., Söling, M., Schneider, A., Gebauer, W. & Harris, J.R. (1991) The role of two distinct subunit types in the architecture of keyhole limpet hemocyanin (KLH). *Naturwissenschaften* **78**, 512–514.
- Harris, J.R., Cejka, Z., Wegener-Strake, A., Gebauer, W. & Markl, J. (1992) Two-dimensional crystallization, transmission electron microscopy and image processing of keyhole limpet hemocyanin (KLH). *Micron Microsc. Acta* **23**, 287–301.
- Harris, J.R., Gebauer, W. & Markl, J. (1993) Immunoelectron microscopy of hemocyanin from the keyhole limpet (*Megathura crenulata*): a parallel subunit model. *J. Struct. Biol.* **111**, 96–104.
- Gebauer, W., Harris, J.R., Heid, H., Söling, M., Hillenbrand, R., Söhlgen, S., Wegener-Strake, A. & Markl, J. (1994) Quaternary structure, subunits and domain patterns of two discrete forms of keyhole limpet hemocyanin: KLH1 and KLH2. *Zoology* **98**, 51–68.
- Harris, J.R., Gebauer, W., Söhlgen, S. & Markl, J. (1995) Keyhole limpet hemocyanin (KLH): purification of intact KLH1 through selective dissociation of KLH2. *Micron* **26**, 201–212.
- Swerdlow, R.D., Ebert, R.F., Lee, P., Bonaventura, C. & Miller, K.I. (1996) Keyhole limpet hemocyanin: structural and functional characterization of two different subunits and multimers. *Comp. Biochem. Physiol.* **113B**, 537–548.
- Söhlgen, S.M., Stahlmann, A., Harris, J.R., Müller, S.A., Engel, A. & Markl, J. (1997) Mass determination, subunit organization and control of oligomerization states of keyhole limpet hemocyanin (KLH). *Eur. J. Biochem.* **248**, 602–614.
- Harris, J.R., Gebauer, W., Adrian, M. & Markl, J. (1998) Keyhole limpet hemocyanin (KLH): Slow *in vitro* reassociation of KLH1 and KLH2 from *Immunothel®*. *Micron* **29**, 329–339.
- Keller, H., Lieb, B., Altenhein, B., Gebauer, D., Richter, S., Stricker, S. & Markl, J. (1999) Abalone (*Haliotis tuberculata*) hemocyanin type I (HtH1): organization of the ca. 400 kDa subunit, and amino acid sequence of its functional units f, g and h. *Eur. J. Biochem.* **264**, 27–38.
- Albrecht, U. & Markl, J. (1995) Pore cells as a possible site of hemocyanin biosynthesis in the keyhole limpet *Megathura crenulata*. *Verh. Dtsch. Zool. Ges.* **88**, 156.
- Harris, J.R. & Horne, R.W. (1991) Negative staining. In *Electron Microscopy in Biology* (Harris, J.R., ed.), pp. 203–228. IRL Press, Oxford, UK.
- Laemmli, U.K. (1970) Cleavage of structural proteins during the assembly of the head of bacteriophage T4. *Nature* **227**, 680–685.
- Markl, J., Markl, A., Schartau, W. & Linzen, B. (1979) Subunit heterogeneity of arthropod hemocyanins: I. Chelicerata. *J. Comp. Physiol.* **130B**, 283–292.
- Weeke, R. (1973) Crossed immunoelectrophoresis. *Scand. J. Immunol.* **2** (Suppl. 1), 47–56.
- Kroll, J. (1973) Crossed-line immunoelectrophoresis. *Scand. J. Immunol.* **2** (Suppl. 1), 79–81.
- Markl, J. & Winter, S. (1989) Subunit-specific monoclonal antibodies to tarantula hemocyanin, and a common epitope shared with calliphorin. *J. Comp. Physiol.* **159B**, 139–151.
- Fernandez-Patron, C., Calero, M., Collazo, P.R., Garcia, J.R., Madrazo, J., Musacchio, A., Soriano, F., Estrada, R., Frank, R., Castellanos-Serra, L.R. & Mendez, E. (1995) Protein reverse staining: high-efficiency microanalysis on unmodified proteins detected on electrophoresis gels. *Anal. Biochem.* **224**, 203–211.
- Walsh, M.J., McDougall, J. & Wittman-Liebold, B. (1988) Extended N-terminal sequencing of proteins of archaeobacterial ribosomes blotted from two-dimensional gels onto glass fiber and polyvinylidene difluoride membrane. *Biochemistry* **27**, 6867–6876.
- Thompson, J.D., Higgins, D.G. & Gibson, T.J. (1994) CLUSTAL W: improving the sensitivity of progressive multiple sequence alignment through sequence weighting, position-specific gap penalties and weight matrix choice. *Nucleic Acids Res.* **22**, 4673–4680.
- Page, R.D.M. (1996) TREEVIEW: an application to display phylogenetic trees on personal computers. *Computer Appl. Biosci.* **12**, 357–358.
- Lamy, J., Leclerc, J., Sizaret, P.-Y., Lamy, J., Miller, K.I., McParland, R. & van Holde, K.E. (1987) *Octopus dofleini* hemocyanin: structure of the seven-domain polypeptide chain. *Biochemistry* **26**, 3509–3518.
- Preaux, G., Gielens, C. & Lontie, R. (1983) Immunological comparison of the functional units of  $\beta$ -hemocyanin of *Helix pomatia*. In *Structure and Function of Invertebrate Respiratory Proteins* (Wood, E.J., ed.), *Life Chem. Reports* (Suppl. 1), pp. 125–128.
- Idakieva, K., Severov, S., Svendsen, I., Genov, N., Stoeva, S., Beltrami, M., Tognon, G., Di Muro, P. & Salvato, B. (1993) Structural properties of *Rapana thomasi* hemocyanin: isolation, characterization and N-terminal amino acid sequence of two different dissociation products. *Comp. Biochem. Physiol.* **106B**, 53–59.
- Drexel, R., Siegmund, S., Schneider, H.J., Linzen, B., Gielens, C., Preaux, G., Kellermann, J. & Lottspeich, F. (1987) Complete amino acid sequence of a functional unit from molluscan hemocyanin (*Helix pomatia*). *Biol. Chem. Hoppe-Seyler* **368**, 617–635.
- Gielens, C., De Geest, N., Xin, X.-Q., Devreese, B., Van Beeumen, J. & Preaux, G. (1997) Evidence for a cysteine-histidine thioether bridge in functional units of molluscan hemocyanins and isolation of the disulfide bridges in functional units d and g of the  $\beta$ -hemocyanin of *Helix pomatia*. *Eur. J. Biochem.* **248**, 879–888.
- Lommerse, J.P.M., Thomas-Oates, J.E., Gielens, C., Preaux, G., Kamerling, J.P. & Vliegthart, J.F.G. (1997) Primary structure of 21 novel monoantennary and diantennary N-linked carbohydrate chains from  $\alpha$ -hemocyanin of *Helix pomatia*. *Eur. J. Biochem.* **249**, 195–222.
- Senoan, N.M., Landrum, J., Bonaventura, J. & Bonaventura, C. (1981) Hemocyanin of the giant keyhole limpet, *Megathura crenulata*. In *Invertebrate Oxygen Binding Proteins* (Lamy, J. & Lamy, J., eds), pp. 703–717. Dekker, New York, USA.
- Harris, J.R., Gebauer, W., Guderian, F.U.M. & Markl, J. (1997) Keyhole limpet hemocyanin (KLH). I: reassociation from *Immunothel®* followed by separation of KLH1 and KLH2. *Micron* **28**, 31–41.
- Harris, J.R., Gebauer, W., Söhlgen, S.M., Nermut, M., V. & Markl, J. (1997) Keyhole limpet hemocyanin (KLH). II: characteristic reassociation properties of purified KLH1 and KLH2. *Micron* **28**, 43–56.

35. Lambert, O., Boisset, N., Taveau, J.-C., Preaux, G. & Lamy, J.N. (1995) Three-dimensional reconstruction of the  $\alpha_D$  and  $\beta_C$ -hemocyanins of *Helix pomatia* from frozen-hydrated specimens. *J. Mol. Biol.* **248**, 431–448.
36. Lamy, J., You, V., Taveau, J.-C., Boisset, N. & Lamy, J.N. (1998) Intramolecular localization of the functional units of *Sepia officinalis* hemocyanin by immunoelectron microscopy. *J. Mol. Biol.* **284**, 1051–1074.
37. Lambert, O., Boisset, N., Penczek, P., Lamy, J., Taveau, J.-C., Frank, J. & Lamy, J.N. (1994) Quaternary structure of *Octopus vulgaris* hemocyanin. *J. Mol. Biol.* **238**, 75–87.
38. Dewilde, S., Winnepenninckx, B., Arndt, M.H.L., Nascimento, D.G., Santoro, M.M., Knight, M., Miller, A.N., Kerlavage, A.R., Geoghegan, N., Van Marck, E., Liu, L.X., Weber, R.E. & Moens, L. (1998) Characterization of the myoglobin and its coding gene of the mollusc *Biomphalaria glabrata*. *J. Biol. Chem.* **273**, 13583–13592.
39. Adamkewicz, S.L., Harasewych, M.G., Blake, J., Saudek, D. & Bult, C.J. (1997) A molecular phylogeny of the bivalve molluscs. *Mol. Biol. Evol.* **14**, 619–629.
40. Stoeva, S., Idakieva, K., Rachev, R., Voelter, W. & Genov, N. (1997) Amino-terminal oxygen-binding functional unit of the *Rapana thomasiana* Grosse (Gastropoda) hemocyanin: carbohydrate content, monosaccharide composition and amino acid sequence studies. *Comp. Biochem. Physiol.* **117B**, 101–107.
41. Trueman, E.R. & Clarke, M.R. (1985) Evolution. In *The Mollusca*, Vol. 10, pp. 1–491. Academic Press, New York, USA.
42. Gu, X. (1998) Early metazoan divergence was about 830 million years ago. *J. Mol. Evol.* **47**, 369–371.

